Structural characteristics of the B6 phase for a bent-core molecular system observed through the B1-B6 transition

Sungmin Kang,* Seng Kue Lee, Masatoshi Tokita, and Junji Watanabe
Department of Organic and Polymeric Materials, Tokyo Institute of Technology, O-okayama, Meguro-ku, Tokyo 152-8552, Japan
(Received 23 July 2009; published 21 October 2009)

A bent-shaped molecule exhibiting the mesophase sequence of B6-B1 was studied to understand the structural characteristics of the B6 phase compared with those of the B1 phase. A well-oriented sample was prepared in a magnetic field and examined by wide-angle x-ray diffraction measurements through the B6-B1 phase transition. The B6 phase has been considered to show only the (002) reflection, but this B6 phase showed broad scattering just inside the (002) reflection. The broad scattering has an intensity maximum at a very similar position to that of the (101) reflection in B1 and evolves into the well-defined (101) reflection on cooling into B1. Thus, B6 has a similar frustrated structure to B1, but the size of the antidomain in B6 may be dynamically distributed while B1 possesses an antidomain of definite size.

DOI: 10.1103/PhysRevE.80.042703 PACS number(s): 61.30.−v

I. INTRODUCTION

Banana-shaped molecules have fascinated numerous researchers in the liquid crystal field since the discovery of unconventional properties [1] as well as their formation of banana phases. A spontaneous polarization originating from breaking the mirror symmetry of achiral molecules, a spontaneous formation of chiral domains, and an organization of frustrated structures in diverse modes are the features of banana phases broadly known as the B1–B7 phases [2,3]. In this study, we refer to the structural characteristics of the B1 and B6 phases by using a material showing the direct phase transition from B6 to B1.

The B1 phase was first reported by Watanabe and co-workers for the classical banana-shaped molecule P-*n*-O-PIMB and bent-dimer [4,5]. The B1 possesses a two-dimensional (2D) frustrated structure with a centrosymmetrical lattice, which is characterized by showing distinct x-ray diffraction patterns with the (101) reflection as well as the (002) one, but without the (00l) reflection with a spacing corresponding to the molecular length. The 2D frustrated structure [6,7] has been explained as the antidomain structure in which the layered structure is built in a small domain with a definite size of more than 30 Å, but the molecules in adjacent domains slide halfway along the layer normal after 180° rotation around their molecular axes. The origin of such a frustrated antidomain structure is thought to be an escape from spontaneous polarization [6,8,9].

On the other hand, few articles report the B6 phase since it has been observed in certain limited systems with shorter terminal alkyl chain lengths. This phase shows a characteristic x-ray diffraction pattern including two reflections, the outer diffuse scattering of the wide-angle region, and the (002) layer reflection corresponding to half a molecular length [10]. It has also been speculated that it possesses an intercalated structure, as shown in Fig. 1 [2,11]. This structural model is reasonable since electron density modulation of a spacing of half a molecular length can result in a pseudolayer reflection with an index of (002), although the driving force to produce such a curious structure is not yet fully understood.

The B1 and B6 phases appear when the number of carbon atoms (n) in the terminal alkyl chain is small, and in a homologous system the B6→B1→B2 alteration is usually observed with increasing n [10–13]. On the other hand, only a few systems show the B6-B1 phase sequence with decreasing temperature [12–15]. In these systems, it is reported that the (101) reflection of B1 disappears upon transformation to B6, but a detailed x-ray analysis has not been performed for the structural change through the B6-B1 transition. Recently, we found a banana-shaped molecule showing the B6-B1 transition [16]: 3-{4-[N-(4-*n*-alkoxyphenyl)iminomethyl]benzoyloxy}phenyl 4-(4-*n*-alkoxybenzoyloxy)benzoate (ASY4S4E, Scheme 1).

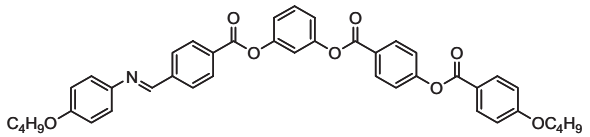

Scheme 1

II. MATERIAL AND EXPERIMENT

The details of the synthesis of ASY4S4E will be published elsewhere [16]. The substance shows the sequence of

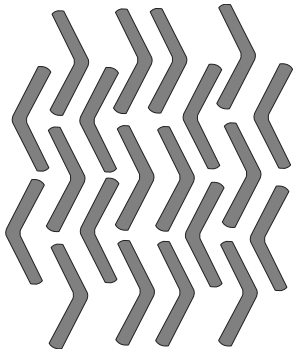

FIG. 1. Intercalated structure proposed for the B6 phase.

*Corresponding author; skang@polymer.titech.ac.jp

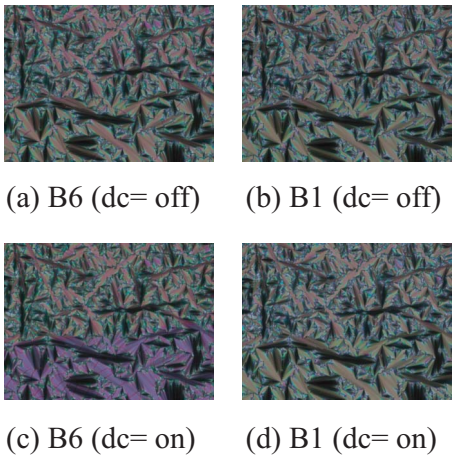

FIG. 2. (Color online) Polarizing optical microscopy textures observed in B6 (a and c) and B1 (b and d) phases upon application of a dc voltage of 40 V to a 4.9 μm-thick cell: (a) and (b) are the OFF state, while (c) and (d) are the ON state. Only a birefringence change was detected between the ON and OFF states in the B6 phase. The electrode is bottom half area of the picture.

Iso-166 °C (14.9 kJ mol^{-1})-B6-150 °C (0.3 kJ mol^{-1})-B1-130 °C (14.0 kJ mol^{-1})-Cr upon the cooling process.

Differential scanning calorimetric (DSC) measurements were carried out with a Perkin Elmer Pyris 1 at a scanning rate of 10 °C min^{-1}. Wide-angle x-ray diffraction (WAXD) measurements were performed using a Rigaku RINT-2500 x-ray generator with monochromic Cu Kα radiation from a graphite crystal monochromator and flat-panel imaging plate. Through the observation of the WAXD patterns for the aligned sample in a magnetic field (5 T), we observed the structural characteristics of the B6 phase in comparison with those of the B1 phase. Optical microscopic textures of materials were examined using an Olympus BX50 polarizing optical microscope (POM) equipped with a temperature-controlled Mettler Toledo FP82 hot stage.

III. RESULTS AND DISCUSSION

As can be confirmed from the results of DSC measurements, a small but recognizable peak is characteristic of the B6-B1 phase transition. The small enthalpy change of 0.3 kJ mol^{-1} suggests that there is only a relatively subtle structural difference between the B6 and B1 phases, as reported previously [12–15].

As observed using a polarized optical microscope, B6 appears as a bâtonnet and coalesces into a fan-shaped texture [11]. Upon transformation into B1 with cooling, the fan-shaped texture is still retained without significant change [12,13]. It should be noted that the fan-shaped texture of B1 observed here is intrinsically different from the typical mosaiclike texture of B1 observed that appears directly from the isotropic melt [2,4]. A detectable difference in nature between the B1 and B6 phases can only be seen when an external electric field is applied. Figure 2 shows the textures of B6 and B1 when a dc voltage of 8 V μm^{-1} was applied. B6 shows a significant change in birefringence while B1 does not respond at all. Switching is not due to the ferroelectric response, but to a dielectric response; initially, the bent axis lies parallel to the polyimide-coated glass plate, but it becomes perpendicular to the plate in an electric field.

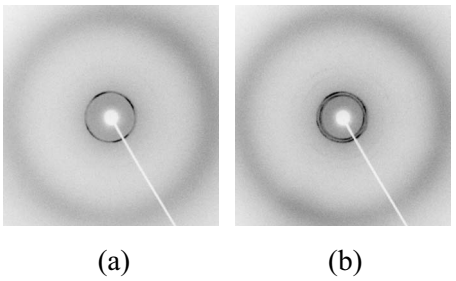

FIG. 3. WAXD profiles of a nonoriented sample in (a) B1 and (b) B6 phases.

One structural characteristic can be speculated upon from the powder x-ray pattern in Fig. 3. Although the broad outer reflection with a spacing of 4.5 Å is commonly observed for both B6 and B1, the inner reflection profile markedly differs between the two. B1 shows two inner reflections with spacings of 19.3 Å and 17.6 Å, which can be assigned to the (101) and (002) reflections of the 2D frustrated lattice, respectively. On the other hand, B6 shows only, the (002) reflection with a spacing of 17.6 Å. It is thus apparent that the (101) reflection of B1 disappears upon transformation to B6 as has been reported [12,15].

To investigate the detailed structure of B6 and the structural change upon B1-B6 phase transition, we have performed a WAXD measurement for an aligned sample. Alignment of samples was accomplished as follows. First, an isotropic droplet with a thickness of ~0.5 mm was placed on freshly rinsed glass plate. Surface anchoring forces the molecules to align with the bent axis perpendicular to the glass plate upon cooling to B6. When the magnetic field (5 T) is simultaneously applied parallel to the glass plate, uniaxial alignment of molecules is achieved such that the long axes of the molecules lie parallel to the field. The applied cooling rate was 1 °C min^{-1} from the isotropic melt.

X-ray diffraction patterns were examined by two different incidences of x-ray beam, which are normal to the direction of the magnetic field but parallel and normal to the glass plate. The reproducible x-ray patterns are obtained on heating and cooling cycles through the B1-B6 phase transition and their typical patterns are shown in Fig. 4. Here, Figs. 4(a) and 4(b) are images taken with the beam parallel to the glass plate, while Figs. 4(c) and 4(d) are images taken with the beam perpendicular to the plate. In Fig. 4(a), one can see two strong inner reflections equidistant along the equatorial line, which is parallel to the magnetic field. These two peaks provide interplanar spacings of 17.6 Å and 8.7 Å, which correspond to the (002) and (004), respectively. Just inside the (002) reflection, four spotlike (101) reflections with a spacing of 19.3 Å are observed. In a vertical direction to the outer region, there is a typical diffuse halo with a spacing of 4.5 Å, which is reminiscent of liquidlike packing of molecules within a layer. All these profiles are characteristic of identify the 2D frustrated B1 structure. On heating to B6, a significant change can be detected only for the (101) reflec-

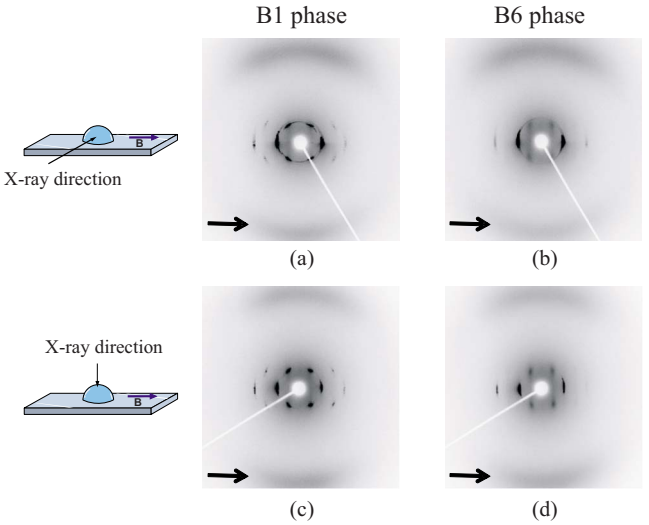

FIG. 4. (Color online) WAXD profiles for the aligned B1 (a, c) and B6 (b, d) phases. The x-ray beam is irradiated parallel (a, b) and normal (c, d) to the glass plate. The arrows on the photographs indicate the direction of the magnetic field.

tion, as shown in Fig. 4(b); the (101) reflection is altered to a broad streak, although its most intense position remains unchanged from that of the (101) reflection of B1.

Similar results are obtained from the profiles with the normal incidence to glass plate, as shown in Figs. 4(c) and 4(d). By comparing Fig. 4(c) with Fig. 4(a) for B1, however, one

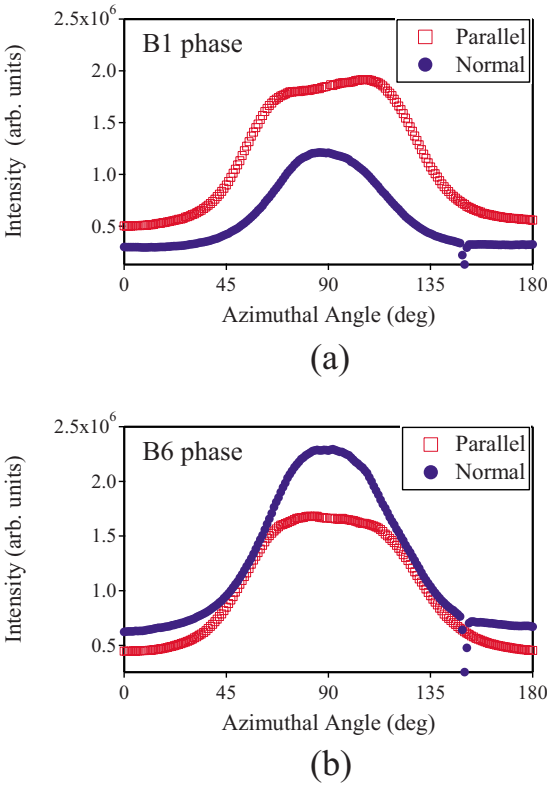

FIG. 5. (Color online) Comparison of β-scan profiles of outer diffuse halos in (a) B1 and (b) B6 phases with parallel (red open square) and normal (blue solid circle) beam incidences.

TABLE I. Ratios of scattering intensity $I(101)$ to $I(002)$ in both B6 and B1 phases for both experimental incidence geometries.

Phase	Incidence direction	Intensity ratio $I(101)/I(002)$
B6	Parallel	0.038
	Normal	0.050
B1	Parallel	0.122
	Normal	0.339

can find a small but significant difference in the intensity profiles between the normal and parallel incidences. First, there is a notable difference in the β-scan profile of the outer halo. This can be clearly seen in Fig. 5; the outer halo in the parallel-incidence profile is expanded more along the azimuthal direction than that of the normal-incidence profile. In other words, the splitting into two intensity maxima, which are derived from the tilted association of side wing moieties of bent molecules, is more marked in the parallel-incidence profile [17–19]. Thus, the molecules tend to align with their bent axes perpendicular to the glass plate because of surface anchoring, although the orientation is not perfect.

Second, we can find the difference in the intensity ratio of $I(101)/I(002)$ between the two incidence geometries. As listed in Table I, the ratios are 0.12 in the parallel-incidence profile and 0.34 for the normal-incidence one. The large ratio for the normal-incidence profile indicates that the 2D frustration preferentially takes place along the glass surface. From

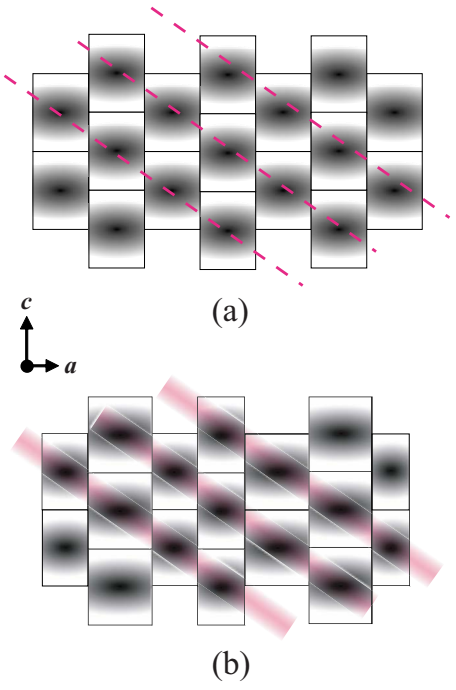

FIG. 6. (Color online) Possible structure models for the B1 and B6 phases. The black and white contrast indicates the electron density distribution of banana-shaped molecules. Oblique pink (a) dotted line and (b) shadows indicate the electron density distribution along the (101) direction, which is more vivid in the B1 phase. Directions a and c indicate lattice axes.

the combined results of diffraction profiles for outer and inner reflections, it can be concluded that the 2D frustration (i.e., antidomain structure) is formed in a direction perpendicular to the molecular bent plane for the B1 and B6 phases. This preferential direction of frustration is similar to that observed in other molecular systems [17–19]. The 2D frustrated structure is shown in Fig. 6(a). The lattice parameters of B1 are $a=23.1$ Å and $c=35.2$ Å, i.e., the antidomain size is 23.1 Å. The same argument can be made for B6 [Fig. 5(b) and Table I], but the alteration of the sharp (101) reflection to diffuse scattering shows that the B6 structure is a type of pseudo-2D frustration. As shown in Fig. 6(b), the antidomain structure obviously exists, but its size is not definite, and it fluctuates from position to position. The average size of the antidomain in B6 is reproducible whenever the cooling condition from the isotropic melt is varied. This suggests that the frustration may occur dynamically to achieve the thermodynamically stable size of the antidomain. The dielectric response preferentially observed for B6 may be allowed owing to this dynamic 2D frustration. Furthermore, it should also be noted that the antidomain size of B1 remains unchanged within the wide liquid crystal (LC) regime of B1 and B6 including the transition temperature.

Finally, we report the size of the antidomain of the B1 phase. Generally, it appears to be larger than 40 Å when B1 is formed directly from the isotropic phase. The size of the system described herein is markedly smaller than this value. This may arise because the preceding B6 phase has a smaller antidomain size.

IV. CONCLUSION

In conclusion, the detailed structure of the B6 phase was investigated by WAXD measurement using an oriented sample through the B1-B6 phase transition. Observation of the (101) reflection together with the (002) reflection clearly shows that the B1 phase has a frustrated structure with a definite 2D lattice. The frustration occurs in a direction perpendicular to the molecular bending plane, which is consistent with the results for other banana-shaped molecular systems [16,19]. Upon transformation to the B6 phase, the (101) reflection is altered to a diffuse streak, but the position of its maximum intensity is the same as that of the (101) reflection of the B1 phase. Thus, the pseudo-2D lattice of B6 is similar to that of B1, but the order of the 2D structure is weak. The frustration in the higher temperature B6 phase may possibly occur dynamically.

ACKNOWLEDGMENTS

This research was supported by a Grant-in-Aid for Creative Scientific Research and a Grant-in-Aid for Young Scientists B (Grant No. 21750138) from the Ministry of Education, Culture, Sports, Science and Technology in Japan.

[1] T. Niori, T. Sekine, J. Watanabe, T. Furukawa, and H. Takezoe, J. Mater. Chem. **6**, 1231 (1996).
[2] G. Pelzl, S. Diele, and W. Weissflog, Adv. Mater. **11**, 707 (1999).
[3] H. Takezoe and Y. Takanishi, Jpn. J. Appl. Phys. **45**, 597 (2006).
[4] J. Watanabe, T. Niori, T. Sekine, and H. Takezoe, Jpn. J. Appl. Phys. **37**, L139 (1998).
[5] T. Sekine, T. Niori, M. Sone, J. Watanabe, S. W. Choi, Y. Takanishi, and H. Takezoe, Jpn. J. Appl. Phys., Part 1 **36**, 6455 (1997).
[6] Y. Nakata, K. Shimizu, and J. Watanabe, J. Phys. II **4**, 581 (1994).
[7] Y. Nakata and J. Watanabe, Polym. J. (Tokyo, Jpn.) **29**, 193 (1997).
[8] J. Prost, Adv. Phys. **33**, 1 (1984).
[9] T. Izumi, T. Niori, Y. Shimbo, Y. Takanishi, H. Takezoe, and J. Watanabe, J. Phys. Chem. B **110**, 23911 (2006).
[10] W. Weissflog, I. Wirth, S. Diele, G. Pelzl, H. Schmalfuss, T. Schoss, and A. Wurflinger, Liq. Cryst. **28**, 1603 (2001).
[11] D. Shen, S. Diele, G. Pelzl, I. Wirth, and C. Tschierske, J. Mater. Chem. **9**, 661 (1999).
[12] J. C. Rouillon, J. P. Macerou, M. Laguerre, H. T. Nguyen, and M. F. Achard, J. Mater. Chem. **11**, 2946 (2001).
[13] H. N. S. Murthy and B. K. Sadashiva, Liq. Cryst. **29**, 1223 (2002).
[14] R. A. Reddy and B. K. Sadashiva, J. Mater. Chem. **14**, 1936 (2004).
[15] R. A. Reddy, B. K. Sadashiva, and V. A. Raghunathan, Chem. Mater. **16**, 4050 (2004).
[16] S. Kang, S. K. Lee, X. Li, M. Tokita, and J. Watanabe, Chem. Lett. **38**, 852 (2009).
[17] Y. Takanishi, H. Takezoe, J. Watanabe, Y. Yakahashi, and A. Iida, J. Mater. Chem. **16**, 816 (2006).
[18] Y. Takanishi, M. Toshimitsu, M. Nakata, N. Takada, T. Izumi, K. Ishikawa, H. Takezoe, J. Watanabe, Y. Takahashi, and A. Iida, Phys. Rev. E **74**, 051703 (2006).
[19] S. Kang, M. Tokita, Y. Takanishi, H. Takezoe, and J. Watanabe, Phys. Rev. E **76**, 042701 (2007).